

HOSTED BY



ELSEVIER

Contents lists available at ScienceDirect

China University of Geosciences (Beijing)

Geoscience Frontiers

journal homepage: [www.elsevier.com/locate/gsf](http://www.elsevier.com/locate/gsf)

Research paper

## Seeing through the magnetite: Reassessing Eoarchean atmosphere composition from Isua (Greenland) $\geq 3.7$ Ga banded iron formations

Allen P. Nutman<sup>a,\*</sup>, Vickie C. Bennett<sup>b</sup>, Clark R.L. Friend<sup>c</sup><sup>a</sup> GeoQuEST Research Centre, School of Earth and Environmental Sciences, University of Wollongong, Wollongong, NSW 2522, Australia<sup>b</sup> Research School of Earth Sciences, Australian National University, Canberra, ACT 0200, Australia<sup>c</sup> Glendale, Tiddington, Oxon, OX9 2LQ, UK

## ARTICLE INFO

## Article history:

Received 24 November 2016

Received in revised form

22 February 2017

Accepted 24 February 2017

Available online xxx

Handling Editor: Christopher J Spencer

## Keywords:

Banded iron formation

Eoarchean

Early atmosphere

Greenalite

Magnetite

## ABSTRACT

Estimates of early atmosphere compositions from metamorphosed banded iron formations (BIFs) including the well-studied  $\geq 3.7$  BIFs of the Isua supracrustal belt (Greenland) are dependent on knowledge of primary versus secondary Fe-mineralogical assemblages. Using new observations from locally well preserved domains, we interpret that a previously assumed primary redox indicator mineral, magnetite, is secondary after sedimentary Fe-clays (probably greenalite)  $\pm$  carbonates. Within  $\sim 3.7$  Ga Isua BIF, pre-tectonic nodules of quartz + Fe-rich amphibole  $\pm$  calcite reside in a fine-grained ( $\leq 100 \mu\text{m}$ ) quartz + magnetite matrix. We interpret the Isua nodule amphibole as the metamorphosed equivalent of primary Fe-rich clays, armoured from diagenetic oxidative reactions by early silica concretion. Additionally, in another low strain lacunae,  $\sim 3.76$  Ga BIF layering is not solid magnetite but instead fine-grained magnetite + quartz aggregates. These magnetite + quartz aggregates are interpreted as the metamorphosed equivalent of Fe-clay-rich layers that were oxidised during diagenesis, because they were not armoured by early silicification. In almost all Isua BIF exposures, this evidence has been destroyed by strong ductile deformation. The Fe-clays likely formed by abiotic reactions between aqueous  $\text{Fe}^{2+}$  and silica. These clays along with silica  $\pm$  carbonate were deposited below an oceanic Fe-chemocline as the sedimentary precursors of BIF. Breakdown of the clays on the sea floor may have been by anaerobic oxidation of  $\text{Fe}^{2+}$ , a mechanism compatible with iron isotopic data previously published on these rocks. The new determinations of the primary redox-sensitive Fe-mineralogy of BIF significantly revise estimates of early Earth atmospheric oxygen and  $\text{CO}_2$  content, with formation of protolith Fe-rich clays and carbonates compatible with an anoxic Eoarchean atmosphere with much higher  $\text{CO}_2$  levels than previously estimated for Isua and in the present-day atmosphere.

© 2017, China University of Geosciences (Beijing) and Peking University. Production and hosting by Elsevier B.V. This is an open access article under the CC BY-NC-ND license (<http://creativecommons.org/licenses/by-nc-nd/4.0/>).

## 1. Introduction

The redox-sensitive Fe-mineralogy of banded iron formations (BIFs) has been used to constrain early Precambrian atmosphere composition and explore the antiquity of metabolic pathways (e.g., Cloud, 1973; Harder, 1978; Holland, 1984; Konhauser et al., 2002, 2007, 2009; Dauphas et al., 2004; Ohmoto et al., 2004, 2014; Johnson et al., 2008; Bekker et al., 2010; Rosing et al., 2010; Li et al.,

2013; Rasmussen et al., 2013). However, redox conditions change during diagenesis and metamorphism, thus Fe-phases now present in BIFs need not reflect conditions when the precursor sediments were deposited (LaBerge, 1964; French, 1973; Rasmussen et al., 2013, 2017).

Detailed micro-petrographic studies of undeformed and non- to weakly-metamorphosed Paleoproterozoic and late Neoproterozoic BIFs from North America, Western Australia and South Africa demonstrate that the oxides magnetite and hematite are diagenetic phases, derived from sedimentary precursor Fe-rich clay silicate minerals  $\pm$  carbonate (e.g., LaBerge, 1964; Ayres, 1972; Dimroth and Chauvel, 1973; Rasmussen et al., 2013, 2017). This means that even

\* Corresponding author.

E-mail address: [anutman@uow.edu.au](mailto:anutman@uow.edu.au) (A.P. Nutman).

Peer-review under responsibility of China University of Geosciences (Beijing).

<http://dx.doi.org/10.1016/j.gsf.2017.02.008>1674-9871/© 2017, China University of Geosciences (Beijing) and Peking University. Production and hosting by Elsevier B.V. This is an open access article under the CC BY-NC-ND license (<http://creativecommons.org/licenses/by-nc-nd/4.0/>).

for best-preserved, non-metamorphosed magnetite or hematite BIF, their present oxide-rich mineralogy cannot be used at face value as a proxy for ocean-atmosphere chemistry (Posth et al., 2008).

For the very ancient ( $\geq 3.7$  Ga) Eoarchean BIFs of the Isua supracrustal belt (Greenland; Moorbath et al., 1973) considered here, the diagenetic assemblages were replaced by new minerals crystallized during high grade metamorphism (500–600 °C) and ductile deformation (Nutman et al., 1984; Dymek and Klien, 1988). Associated with this high-grade tectonothermal crystallisation is the loss of microscopic diagenetic textures, and in nearly all localities, loss of mesoscopic sedimentary structures as well (Fig. 1; Nutman et al., 2007). This is an extra barrier to use the mineralogy of these Eoarchean BIFs as proxies to constrain environmental conditions at near the start of Earth's sedimentary record. This paper reports the textures and mineralogy from rare low strain domains in Isua BIF that indicate significant removal of iron from the hydrosphere was first as  $\text{Fe}^{2+}$  in clay minerals. This has ramifications for using the magnetite in these BIFs to constrain the composition of the early atmosphere (Fig. 2).

## 2. Banded iron formations of the Isua supracrustal belt

The Isua supracrustal belt of southern West Greenland contains the world's largest accumulation of Eoarchean BIF (Moorbath et al., 1973; Appel, 1980; Dymek and Klein, 1984; Frei and Polat, 2007; Nutman et al., 2009) and is the prime focus for constraining environmental conditions near the start of the sedimentary record. On the bulk scale, metamorphism of many Isua BIFs was essentially isochemical, such that they preserve seawater-like rare earth element + yttrium (REE + Y) signatures and high Ni/Fe (Bolhar et al., 2004; Konhauser et al., 2009). Additionally, the international reference BIF material (IF-G) which comes from Isua, preserves this seawater-like signature (Friend et al. 2007).

Most of the layering in Isua BIFs is thin, with separation of quartz and magnetite  $\pm$  amphibole into distinct anastomosing mesobands (Fig. 1). This tectonic fabric was produced by the destruction and transposition of original sedimentary layering during strong ductile deformation under amphibolite facies conditions, combined with metamorphic segregation of quartz and the recrystallization of Fe-bearing phases, mainly to magnetite. However, in the rare low strain domains described here, preserved Isua BIF sedimentary layering, nodular diagenetic structures and mineralogical-textural

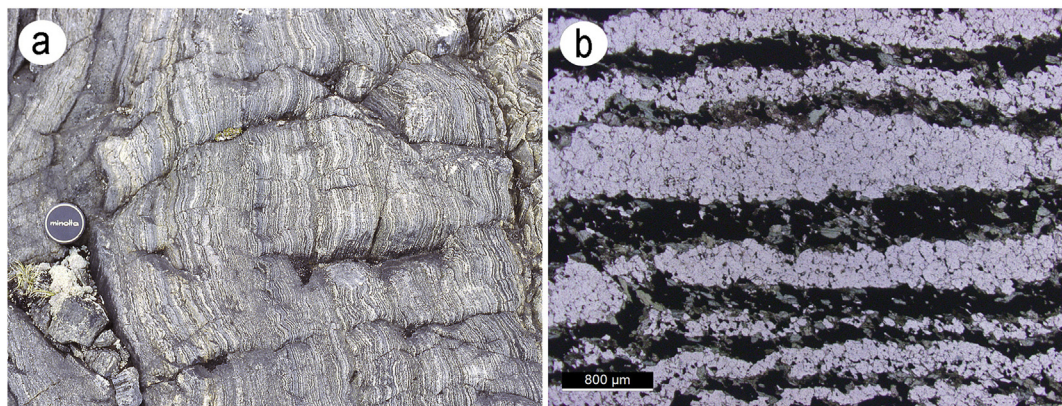


**Figure 1.** (a) Typical outcrop of Isua strongly deformed quartz + magnetite + amphibole BIF, with fine-scale mostly magnetite versus mostly quartz layering. Due to the degree of deformation this layering no longer reflects any sedimentary structure. (b) Transmitted light photomicrograph of strongly deformed Isua BIF. Note that the magnetite (black) + Fe-rich amphibole (green) occurs as discrete layers, *not* intergrown with quartz (translucent).

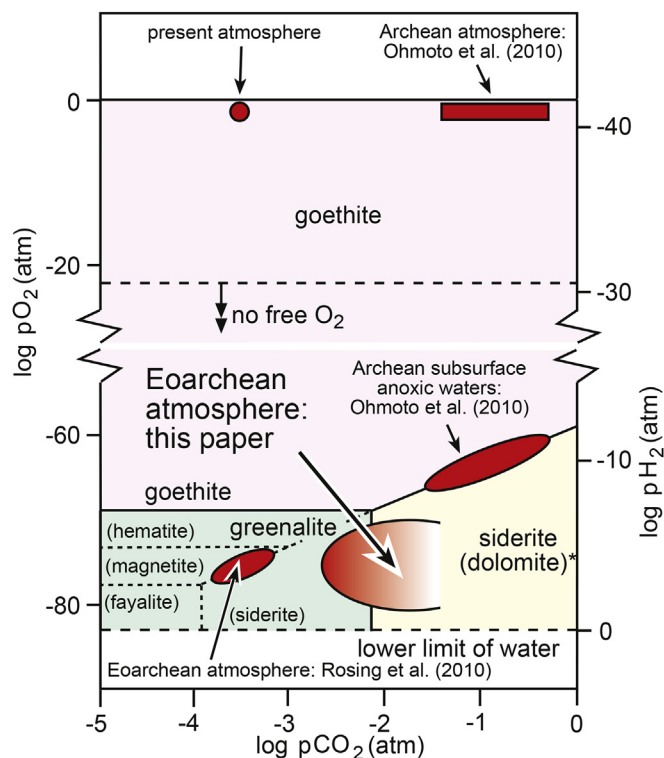


**Figure 2.** Mineralogical stabilities under different oxygen and carbon dioxide concentrations from Ohmoto et al. (2004), showing the Eoarchean atmosphere conditions proposed in this paper, by Rosing et al. (2010), and atmospheric and deep water conditions proposed by Ohmoto et al. (2004). Siderite (dolomite)\* refers to the evidence presented by Klien and Bricker (1977) that addition of Ca and Mg to the system gives rise to dolomite instead of siderite.

relationships provide evidence that Fe-oxides were not the primary depositional phases.

In a low strain lens (65°12.405'N, 49°45.661'W; GPS datum WGS84) in the >1 km thickness of folded ~3.7 Ga 'Iron Mountain' BIF at the eastern end of the Isua supracrustal belt (Moorbath et al., 1973; Dymek and Klien, 1984; Nutman et al., 2009), pre-tectonic siliceous nodules reside in a fine-grained magnetite + quartz matrix over the <5 m extent of an outcrop (Fig. 3a,b). The nodules consist of quartz + Fe-rich amphibole + accessory calcite  $\pm$  accessory magnetite as a dusting

of disseminated 5–10  $\mu\text{m}$  grains (Fig. 3c). Thin magnetite veins traverse the nodule margins, indicative of secondary oxidation (Fig. 4a). We interpret the nodules as a metamorphosed analogue of the silica concretions formed during diagenesis of late Neoproterozoic–early Paleoproterozoic BIF, where patchy early silica cementation protected primary Fe-clay  $\pm$  carbonate minerals from extensive oxidation and also the sedimentary structure from compaction (Rasmussen et al., 2013). The Isua nodule matrix is a fine-grained aggregate of magnetite + quartz (Fig. 4b,c), with the magnetite containing micron-scale inclusions of Fe–Mg silicate (amphibole?) and quartz (Fig. 5a). In other ‘Iron

Mountain’ BIF low strain lacunae sedimentary layering is preserved, albeit distorted by folding (Frei and Polat, 2007). In such cases, layers are never entirely iron oxide, with always  $\geq 20$  wt.%  $\text{SiO}_2$  (Frei and Polat, 2007), which is compatible with the Fe-rich sedimentary layering reflecting post-depositional oxidation of Fe-clays giving rise to Fe-oxide + silica aggregates.

The second example presented in this paper is from the  $\sim 3.76$  Ga *dividing sedimentary unit*, which separates the southern  $\sim 3.8$  Ga and northern  $\sim 3.7$  Ga portions of the Isua supracrustal belt (Nutman et al., 2009). Within a  $< 2$  m long low strain domain ( $65^\circ 09.870' \text{N}$ ,  $49^\circ 48.934' \text{W}$ ) the layering is on a centimetre rather

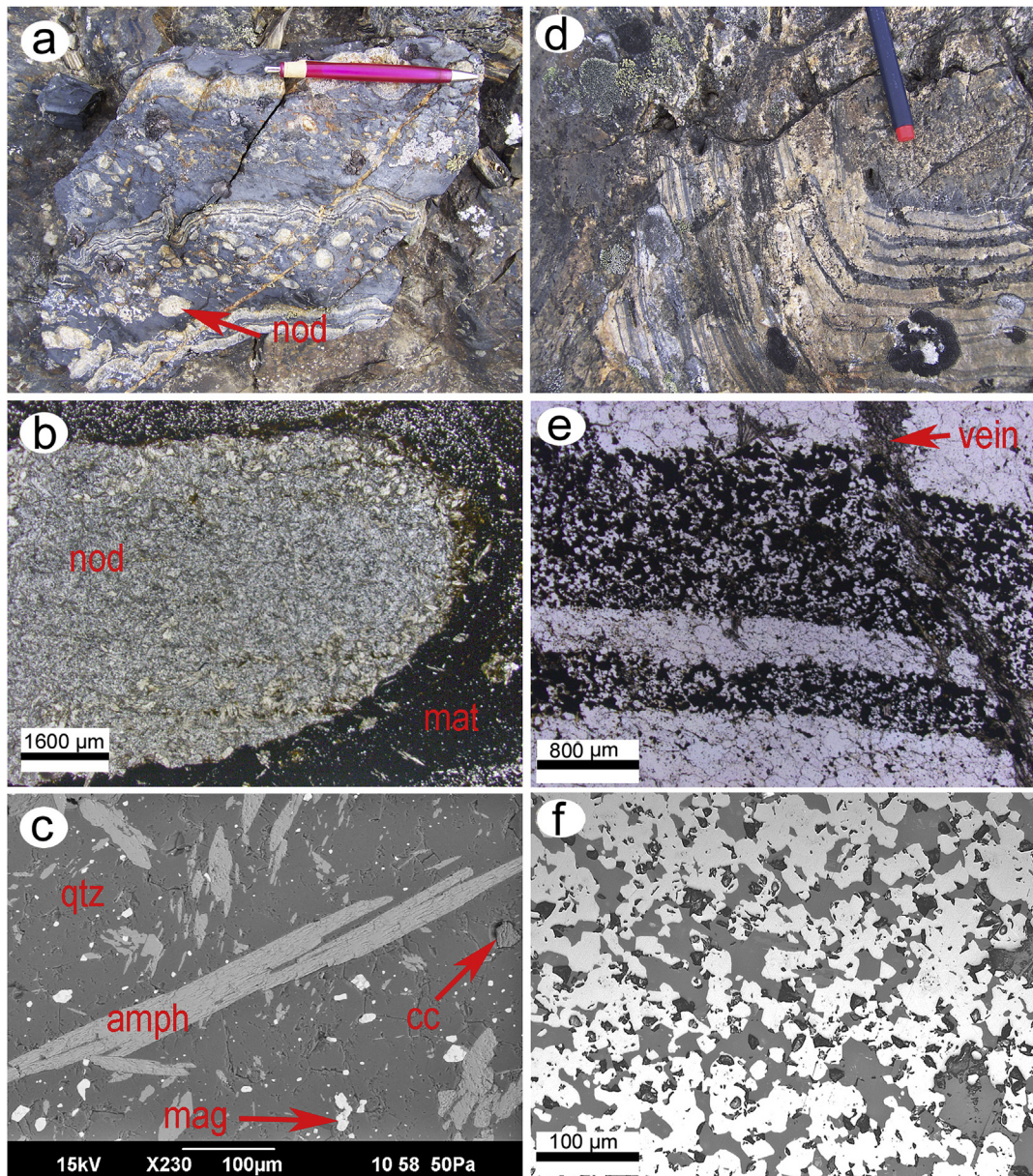


**Figure 3.** (a) Sedimentary-diagenetic siliceous nodules (nod) within  $\sim 3.7$  Ga Isua ‘Iron Mountain’ BIF (WGS84 GPS;  $65^\circ 12.405' \text{N}$ ,  $49^\circ 45.661' \text{W}$ ). (b) Photomicrograph of a nodule. Matrix of quartz + magnetite (mat) aggregate surrounds a nodule of quartz + Fe-rich amphibole  $\pm$  calcite with minor disseminated magnetite (nod). (c) SEM back scatter electron image of interior of a nodule. Quartz (qtz) and Fe-rich amphibole (amph) are the dominant phases, together with minor calcite (cc) and accessory disseminated mag (mag). (d) Low deformation lacuna within  $\sim 3.76$  Ga Isua *dividing sedimentary unit* BIF ( $65^\circ 09.881' \text{N}$ ,  $49^\circ 48.853' \text{W}$ ). On the right side there is broader sedimentary layering preserved. On the left side deformation is high, with transposed compositional layering overprinted by a magnetite foliation. (e) Transmitted light photomicrograph of Fig. 3d low strain BIF showing that the magnetite-rich layers consist of fine-grained aggregates of magnetite + quartz. An amphibole vein (vein) developed by reduction of magnetite + quartz due to fluid introduced in a metamorphic event. (f) Reflected light photomicrograph of magnetite-bearing layers, showing that they consist of a 100–50  $\mu\text{m}$  granoblastic aggregate of quartz (dull on image) and magnetite (bright on image).

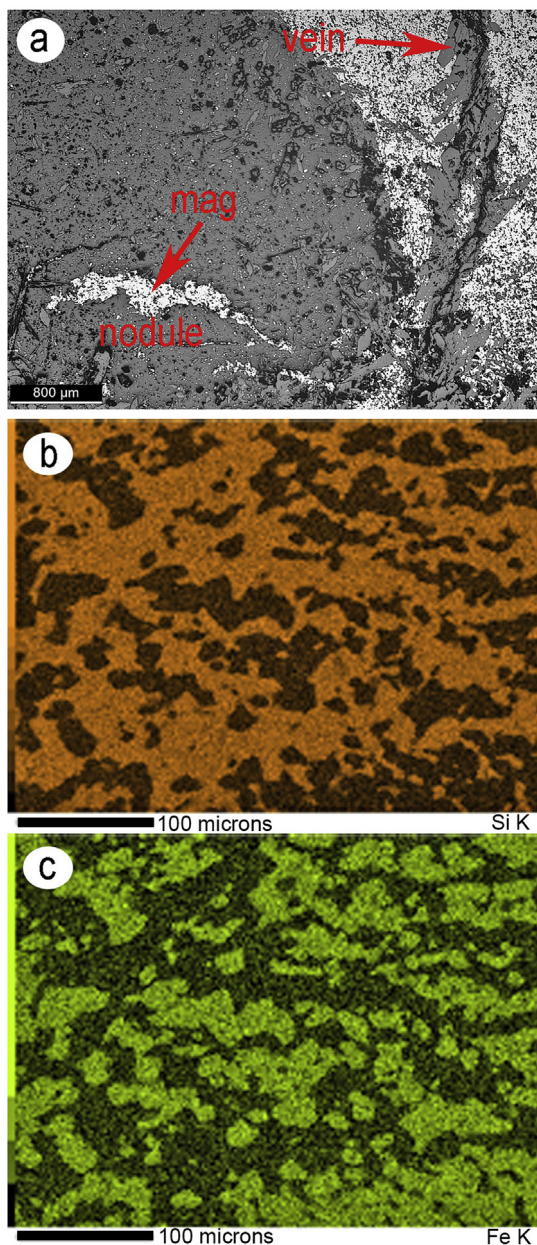


**Figure 4.** (a) Reflected light image of a secondary magnetite-rich (mag) vein traversing interior of quartz-rich nodule (left hand side of image). Note also the discordant vein (vein) in the right hand side of the image, where passage of later reducing fluids transformed the fine-grained quartz + magnetite matrix into coarser-grained Fe-rich amphibole. (b) SEM silicon map of nodule matrix. (c) SEM iron map of nodule matrix.

than millimetre scale, locally graded and is of a similar magnitude to the layering observed in Earth's oldest (~3.5 Ga) non-metamorphosed and undeformed chemical sedimentary rocks in the Pilbara, Western Australia (Van Kranendonk et al., 2003). At the margin of the low strain domain (Fig. 3d left hand side), sedimentary layering is transposed, thinned and overprinted by a much coarsened, granular magnetite–quartz banding. Where sedimentary layering is preserved (Fig. 3d right hand side), the quartz layers contain a dusting of fine-grained (~5–10 μm) disseminated magnetite, whereas the interspersed Fe-rich layers are fine-grained aggregates of quartz + magnetite (Fig. 3e,f). The magnetite contains rare, small quartz and amphibole inclusions (Fig. 5b). Consistent

with observations from the low strain domain in the ~3.7 Ga 'Iron Mountain' BIF, this again indicates that the magnetite was not derived from recrystallization of massive sedimentary Fe-hydroxide layers, but could be from post-depositional breakdown of Fe-silicate (clay) to give quartz + Fe-oxide.

Magnetite in Isua BIF contains ~0.5 wt.% SiO<sub>2</sub> (Table 1). Silician magnetite is a feature of diagenetic magnetite in non-metamorphosed BIF (Huberty et al., 2012). The magnetite in the undeformed Isua BIF layers contains up to ~500 ppm sulfur and 60–80 ppm Ni (Table 1), yet these best-preserved BIF are free of separate sulphide phases. Conversely, strongly-deformed Isua BIF displays some small disseminated pyrite grains (Appel, 1980; Papineau and Mojzsis, 2006). A possibility is that sulphur initially lodged in the magnetite as a nickeliferous greigite component, but some later exsolved to form sulfides during deformation-promoted high-temperature metamorphic recrystallisation.

Eoarchean dolomitic sedimentary carbonates are also encountered in Isua (Bolhar et al., 2004; Nutman et al., 2009, 2010, 2016). These have seawater-like REE + Y trace element signatures, indicating deposition in a marine environment (Nutman et al., 2010), and not from hydrothermal fluids. In a unique low-strain domain in ~3.7 Ga dolomitic rocks (Nutman et al., 2016), shallow water sedimentary structures such as cross-lamination, storm-wave breccias (tempestites) and the world's oldest stromatolites are preserved (Fig. 6). Zircon U–Pb geochronology of rare volcanogenic grains indicate that these shallow water carbonates are coeval with the 'Iron Mountain' BIF (Nutman et al., 2009).

### 3. Discussion

Because of the  $\Delta^{33}\text{S}$  sulfur isotope mass-independent-fractionation signatures (Whitehouse et al., 2005; Papineau and Mojzsis, 2006), an important starting condition for our model is that the Eoarchean atmosphere must have been essentially anoxic. Experimental work (Harder, 1978; Konhauser et al., 2007) demonstrates that under anoxic conditions and consequently a high UV flux, Fe-clays such as greenalite, *not* Fe-hydroxides such as goethite, are produced by photolysis reaction between dissolved Fe<sup>2+</sup> and silica. In addition, other experimental work shows that under anoxic conditions, and even without UV action, there is a propensity for dissolved Fe<sup>2+</sup> and silica to react to form Fe-silicate minerals (Tosca et al., 2016). In their study, Tosca et al. (2006) demonstrated a pathway of first forming nanoparticles of Fe-serpentine, which eventually aggregate to form the mineral greenalite. Thus depending on water Fe/Si ratio, greenalite-rich muds or greenalite-bearing cherts are produced (e.g. Rasmussen et al., 2017). Thus in the Isua anoxic environment, the initial removal of dissolved oceanic iron could have been by this process, with the Fe-rich clays raining down into deeper, lower flow regime water (Fig. 7). In transitional zones, mixed dolomitic–greenalite-bearing lithotypes can be present, as has been observed in well-preserved Neoarchean sequences (e.g. Rasmussen et al., 2017 and references therein). In deeper waters, volcanism replenishes Fe<sup>2+</sup> (Konhauser et al., 2007; Bekker et al., 2010), whereas surficial water undergoes Fe-depletion because of Fe-clay formation within the photic zone. This will be replenished by Fe<sup>2+</sup> from deeper water, probably from volcanic sources (Fig. 7). The implication of removal of oceanic Fe<sup>2+</sup> by these mechanisms is that Isua-time shallow water chemical sedimentary rocks should be less Fe-rich, and this is in accord with the dominance of dolomite rather than Fe-rich minerals in the only instance where Isua chemical sedimentary rocks preserve shallow water sedimentary structures and stromatolites (Fig. 3a,b;

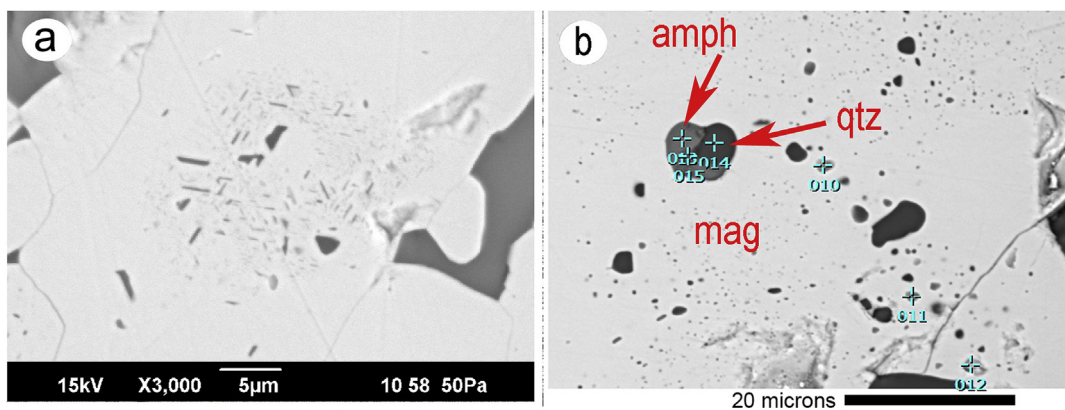


**Figure 5.** (a) Matrix to the nodules shown in Fig. 3a. b. SEM BSE image of micron and sub-micron inclusions of Fe–Mg silicate (probably amphibole from EDS spectra) showing up as dark tabular objects + quartz within matrix magnetite of the nodules shown in Fig. 3. (b) SEM BSE image of micron-scale of amphibole (amph) + quartz (qtz) inclusions in magnetite (mag) within least-deformed BIF in the *dividing sedimentary unit*.

Nutman et al., 2016, 2007). This matches what is observed in early Precambrian chemical sedimentary rocks that are well-preserved, because of minimal metamorphic overprint and tectonic disruption. Thus Rasmussen et al. (2017 and references therein) noted that in the late Archaean Campbellrand carbonate platform (Transvaal Supergroup, South Africa), dolomitic carbonates predominate, whereas associated deeper water facies consist of iron-rich BIF. This scenario of Fe accumulation in deeper waters is consistent with a marine Fe-chemocline of previous BIF genesis models (Bekker et al., 2010). In addition, prior to the evolution of silica-secreting organisms, the oceanic concentration of dissolved silica would have been significantly higher and probably close to or at saturation with respect to amorphous silica (Siever, 1992). Therefore, the inferred composition of most of the ocean during much of the Archaean would have favoured the nucleation and precipitation of hydrous ferrous silicates.

**Table 1**

LA-ICP-MS analyses of magnetite in low strain BIF, dividing sedimentary unit (oxides in wt.%, trace elements in ppm).

Sample	#1	#2	#3	#4	#5	NIST612*	Expected
SiO <sub>2</sub>	0.41	0.42	0.41	0.97	0.47	69.7	69.7
Al <sub>2</sub> O <sub>3</sub>	0.18	0.18	0.19	0.20	0.16	2.01	2.11
CaO	bdl	bdl	bdl	bdl	bdl	11.55	11.83
S	548.5	543.1	537.5	564.6	607.8		
Mg	31.2	31.2	43.5	39.4	23.6	52.49	77.4
Ti	116.8	117.0	108.1	118.6	97.3	40.63	48.1
V	4.49	4.43	4.50	4.44	4.48	37.78	39.22
Cr	4.66	4.76	bdl	16.3	bdl	33.76	39.88
Mn	311.6	310.3	348.6	309.0	298.9	37.37	38.43
Fe	stoch	stoch	stoch	stoch	stoch	97.22	56.33
Ni	70.0	69.4	77.1	79.9	61.3	40.85	38.44
Cu	bdl	bdl	bdl	bdl	bdl	36.59	36.71
Zn	141.1	140.2	146.0	182.7	143.1	40.41	37.92
Y	0.023	bdl	bdl	0.219	0.033	38.12	38.25
La	bdl	bdl	bdl	0.026	0.011	35.24	35.77
Ce	0.031	0.029	bdl	0.036	bdl	37.06	38.35
Pr	bdl	bdl	bdl	0.006	bdl	36.79	37.16
Nd	0.011	0.010	bdl	0.002	bdl	34.71	35.24
Sm	bdl	bdl	bdl	bdl	bdl	36.99	36.71
Eu	0.0031	0.0030	bdl	bdl	bdl	34.71	34.44
Gd	bdl	bdl	bdl	0.015	0.007	36.97	36.95
Tb	bdl	bdl	0.057	bdl	bdl	36.21	35.92
Dy	bdl	bdl	bdl	0.016	bdl	35.02	35.97
Ho	0.002	bdl	bdl	bdl	bdl	37.27	37.87
Yb	0.022	0.024	0.014	0.043	0.013	37.16	39.95
Lu	0.001	0.001	bdl	0.006	bdl	35.99	37.71
Th	0.006	bdl	0.002	0.046	bdl	36.68	37.23
U	0.002	0.002	0.001	0.020	bdl	35.39	37.15

Magnetite data normalised using the stoichiometric amount (wt.%) of iron; NIST612\*: NIST612 glass analysed as unknown, calibrated against NIST610 (69.7 wt.% SiO<sub>2</sub>); NIST expected values from Pearce et al. (1997).

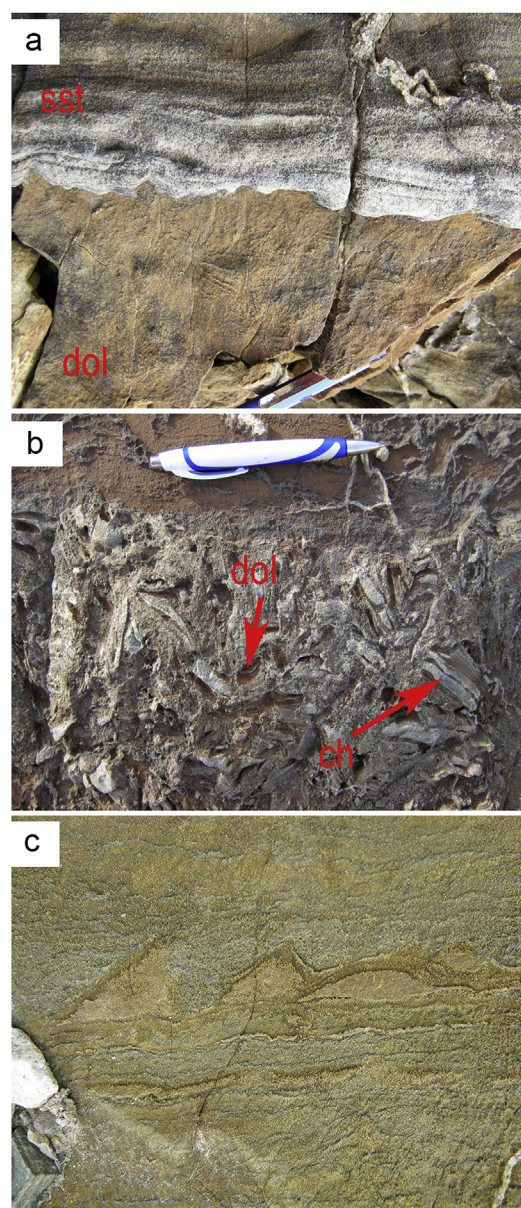


**Figure 6.** (a) Cross-lamination sedimentary structure preserved in 3.7 Ga quartz + dolomite sandstone. Sandstone (sst) overlies a dolostone unit (dol). (b) 3.7 Ga tempestite breccia of chert (ch) and carbonate (dol) clasts in a dolomite + quartz matrix. (c) Rare relict stromatolites preserved in 3.7 Ga dolomitic rocks (see Nutman et al., 2016 for detailed account).

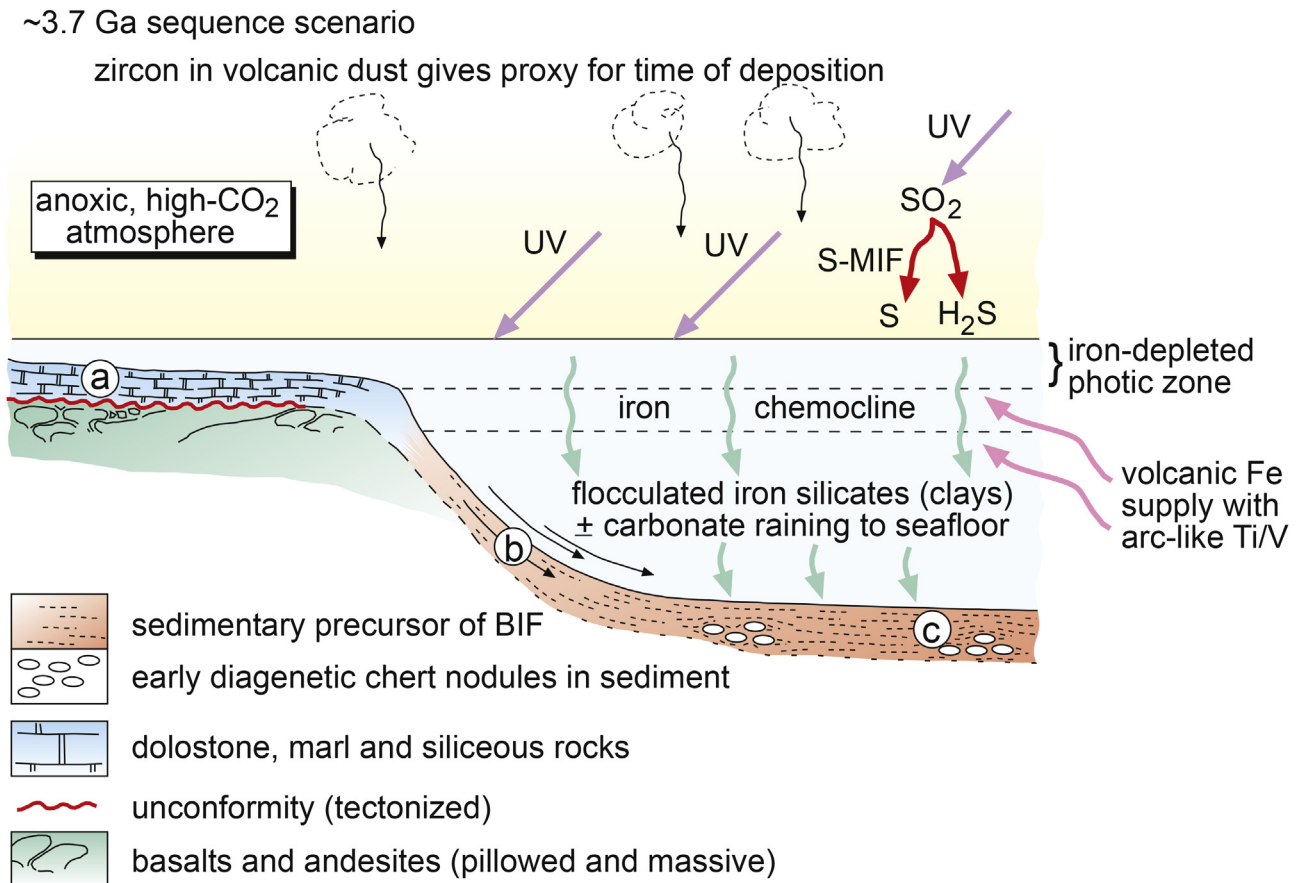


**Figure 7.** Schematic diagram illustrating stages and processes in depositing the sedimentary protoliths of ~3.7 Ga Isua magnetite BIF and their relationship with shallow-water Fe-poor carbonate sedimentary rocks (facies typology modified from Fig. 7c of Bekker et al. (2010)). (a) Above iron chemocline, Fe-poor carbonates + silica deposited in shallow marine environment. There is an unconformity with underlying ~3.71 Ga arc volcanic rocks. (b) Slope transition can supply turbidites (carbonate, clays, silica) into the banded iron formation basin. (c) The protoliths of BIF were dominated by deposition of Fe-clay flakes and silica with silica cement, plus some turbiditic components. On the seabed, if early silica cement is limited, the Fe-clays are converted first to (hydr)oxides + more silica. In later diagenesis and/or metamorphism, these are converted into magnetite + quartz.

Removal of Fe from an anoxic ocean as Fe-clays in an environment of low free oxygen is demonstrated by Fe-rich amphibole in Isua BIF early silica nodules and is consistent with early minnesotaite or greenalite in North American non-metamorphosed BIF and stilpnomelane in weakly-metamorphosed Australian BIF (LaBerge, 1964; Ayres, 1972; Rasmussen et al., 2013). Inspection of the mineral formula for greenalite ( $\text{Fe}_6^{2+}\text{Si}_4\text{O}_{10}(\text{OH})_8$ ) demonstrates that formation of oxides from it does not need an external source of extra oxygen, which would be paradoxical for an anoxic early Earth. Instead it was a redox process involving conversion of some  $\text{Fe}^{2+}$  to  $\text{Fe}^{3+}$ . As observed in Hamersley BIF (Rasmussen et al., 2013), the degree of earliest silica cementation to produce nodules governed whether the diagenetic redox process went to completion. Without this cementation, clay oxidation could advance to completion, giving aggregates of silica and Fe-oxides or hydroxides that during metamorphism recrystallised to fine-grained quartz + magnetite intergrowths (Fig. 3). Conversely, the early silica cementation forming the nodules shielded primary clay minerals from diagenetic oxidation. In the case of Isua, metamorphism converted the primary minerals to Fe-rich amphibole ± calcite (in the silica nodule studied, there were apparently both early Fe-silicate and carbonate minerals based on the present mineralogy of quartz + amphibole + calcite). Hence for Isua BIF, we propose that the oxidation occurred during diagenesis by reactions taking place in soft sediment, shortly after burial, and thus was *unrelated* to the initial removal of iron from the ocean.

Phase diagrams have been used to relate the stability of iron-bearing minerals to  $\rho\text{CO}_2$ ,  $\text{O}_2$  and  $\text{H}_2$ , to derive constraints on their partial pressures in the Archean atmosphere relative to present atmospheric levels (PAL; Fig. 2). These studies give considerably varying estimates, from  $\text{CO}_2$ -rich and oxygen deficient (e.g., Kasting, 2014),  $\text{CO}_2$ - and oxygen-rich (Ohmoto et al., 2004) and specifically for Isua,  $\text{CO}_2$  similar to PAL, but oxygen-poor (Rosing et al., 2010). The concentration of  $\text{CO}_2$  and  $\text{O}_2$  vary considerably with depth in the modern oceans. Therefore, these phase diagrams can only be used for *order of magnitude* constraints on Eoarchean atmospheric conditions. The Rosing et al. (2010) proposal for Eoarchean atmospheric  $\text{CO}_2$  levels within the same order as PAL (i.e.  $<10^{-3}$  bar) was based on magnetite + siderite in Isua BIF reflecting the chemical environment *during* deposition (Fig. 2). The field relationships and detailed petrography presented here suggest that this is unlikely. Furthermore, Rosing et al. (2010) calculated the stability fields for anhydrous mineral phases (Fig. 2). As shown by Ohmoto et al. (2004), introduction of water sees the (anhydrous) Fe-silicate fayalite and the Fe-oxide magnetite becoming metastable, and instead stable phases are (hydrous)  $\text{Fe}^{2+}$  clay minerals such as greenalite and minnesotaite (Fig. 2). In this hydrous system, which is more appropriate for the formation of Isua BIF, the stability field of siderite retreats to higher  $\rho\text{CO}_2$  levels, and is  $\geq \sim 10$  PAL when greenalite is present and  $\geq \sim 100$  PAL when minnesotaite is present (Ohmoto et al., 2004). In the late diagenesis to earliest metamorphism of Neoproterozoic–Palaeoproterozoic BIF, minnesotaite has been observed to form from greenalite (French, 1973), and

experiments by Konhauser et al. (2007) precipitated greenalite from Fe-, Si-saturated water under an anoxic atmosphere and high UV flux. Therefore the  $\geq \sim 10$  PAL for greenalite is considered as a conservative, more realistic constraint for carbonate stabilisation. Addition of  $Mg^{2+}$  and  $Ca^{2+}$  to the  $H_2O-CO_2-Fe-Si$  system replaces siderite by dolomite-ankerite at all oxygen levels (Klien and Bricker, 1977). This is in accord with dolomite-ankerite being the predominant Isua sedimentary carbonate with a seawater-like REE + Y trace element signature (Nutman et al., 2010, 2016). Our petrographic observations on Isua BIFs combined with phase diagrams indicate that Eoarchean  $pCO_2$  (atm) was  $\geq 0.01$  bar ( $>10$  PAL). However, in the Eoarchean, in the absence of other greenhouse gases, approximately 0.2 bar  $CO_2$  would have been required to stop the oceans freezing (Kasting, 1987). Any shortfall of greenhouse gases could have been provided by methane, produced by either methanogens or serpentinization of peridotite (e.g., Sleep et al., 2004).

Anaerobic oxidation of  $Fe^{2+}$  in clays gives rise to magnetite spotting and releases silica (Shelobolina et al., 2012; Pentrákova et al., 2013). We propose this is a strong candidate for a preliminary process in Isua BIF diagenesis.  $\delta^{56}Fe$  values for Isua BIF magnetite of +0.4 to +1.1‰ and for Isua Fe-bearing carbonate of +0.1 to +0.9‰, have been interpreted as evidence for anaerobic oxidation of  $Fe^{2+}$  (Dauphas et al., 2004; Craddock and Dauphas, 2011; Czaja et al., 2013). Our observations are in accord with the isotopic evidence of an oxidative process, but we propose that aqueous Fe was first precipitated as  $Fe^{2+}$ -clays ( $\pm$ carbonate), prior to post-depositional biomediated partial oxidation, eventually to give after metamorphism the observed magnetite + quartz assemblage. Trace sulfur and nickel within Isua BIF magnetite not recrystallised by deformation (Table 1) could reflect primitive greigite-based enzymes (Russell and Hall, 2006) in the oxidative mechanism.

#### 4. Conclusions

- (1) Eoarchean BIF from Isua are in almost all occurrences strongly deformed, and in these rocks the segregation of phases to alternating magnetite-rich and quartz bands is an entirely tectono-metamorphic feature.
- (2) In rare low strain areas, quartz-rich nodules in Isua BIF contain disseminated amphiboles, whereas preserved sedimentary layering consists of 50–100  $\mu m$  aggregates of quartz + magnetite. The nodules are interpreted to reflect sites where early diagenetic silicification protected depositional  $Fe^{2+}$ -clays (greenalite?)  $\pm$  carbonate from diagenetic oxidation. In the sedimentary layering oxidation replaced the  $Fe^{2+}$ -clays by silica + Fe-(hydr)oxide aggregates, subsequently recrystallized to quartz + magnetite during metamorphism.
- (3) Diagenetic oxidation of the  $Fe^{2+}$ -clays could have been by bio-mediation, as observed for modern clays. This mechanism is compatible with previously published Fe-isotope data for Isua BIF.
- (4) Deposition of iron as  $Fe^{2+}$ -clays requires higher  $CO_2$  levels (compared with present atmospheric compositions) in the Eoarchean atmosphere, than have been estimated previously from Isua.

#### Acknowledgements

The project was supported by Australian Research Council (Grant No. DP120100273) and the GeoQuEST Research Centre of the University of Wollongong, Australia. Mitchell Nancarrow of the University of Wollongong Electron Microscopy Centre is thanked for assistance with imaging.

#### References

- Appel, P.W.U., 1980. On the early Archaean Isua banded iron-formation. *Precambrian Research* 11, 73–87.
- Ayres, D.E., 1972. Genesis of iron-bearing minerals in the Brockman Iron Formation mesobands in the Dales Gorge Member, Hamersley Group, Western Australia. *Economic Geology and the Bulletin of the Society of Economic Geologists* 67, 1214–1233. <http://dx.doi.org/10.2113/gsecongeo.67.8.1214>.
- Bekker, A., Slack, J.F., Planavsky, N., Krapež, B., Hofmann, A., Konhauser, K.O., Rouxel, O.J., 2010. Iron formation: the sedimentary product of a complex interplay among mantle, tectonic, oceanic, and biospheric processes. *Economic Geology* 105, 467–508.
- Bolhar, R., Kamber, B.S., Moorbath, S., Fedo, C.M., Whitehouse, M.J., 2004. Characterisation of early Archaean chemical sediments by trace element signatures. *Earth and Planetary Science Letters* 222, 43–60.
- Cloud, P., 1973. Paleocological significance of the banded iron-formation. *Economic Geology* 68, 1135–1143.
- Craddock, P.R., Dauphas, N., 2011. Iron and carbon isotope evidence for microbial iron respiration throughout the Archean. *Earth and Planetary Science Letters* 303, 121–132.
- Czaja, A.D., Johnson, C.M., Beard, B.L., Roden, E.E., Li, W.Q., Moorbath, S., 2013. Biological Fe oxidation controlled deposition of banded iron formation in the ca. 3770 Ma Isua Supracrustal Belt (West Greenland). *Earth and Planetary Science Letters* 363, 192–203.
- Dauphas, N., van Zuilen, M., Wadhwa, M., Davis, A.M., Marty, B., Janney, P.E., 2004. Clues from Fe isotope variations on the origin of early Archaean BIFs from Greenland. *Science* 306, 2077–2080.
- Dimroth, E., Chauvel, J.J., 1973. Petrography of the Sokoman iron formation in part of the central Labrador Trough, Quebec, Canada. *Bulletin of the Geological Society of America* 84, 111–134.
- Dymek, R.F., Klien, C., 1988. Chemistry, petrology and origin of banded iron-formation lithologies from the 3800 Ma Isua supracrustal belt, west Greenland. *Precambrian Research* 39, 247–302.
- Frei, R., Polat, A., 2007. Source heterogeneity for the major components of  $\sim 3.7$  Ga banded iron formations (Isua Greenstone Belt, Western Greenland): tracing the nature of interacting water masses in BIF formation. *Earth and Planetary Science Letters* 253, 266–281.
- French, B.M., 1973. Mineral assemblages in diagenetic and low grade metamorphic iron formation. *Economic Geology* 68, 1063–1074.
- Friend, C.R.L., Bennett, V.C., Nutman, A.P., Norman, M.D., 2007. Seawater trace element signatures (REE+Y) from Eoarchean chemical (meta)sedimentary rocks, southern West Greenland. *Contributions to Mineralogy and Petrology*. <http://dx.doi.org/10.1007/S00410-007-0239-z>.
- Harder, H., 1978. Synthesis of iron layer silicate minerals under natural conditions. *Clays and Clay Minerals* 26, 65–72. <http://dx.doi.org/10.1346/CCMN.1978.0260108>.
- Holland, H.D., 1984. *The chemical evolution of the atmosphere and oceans*. Princeton University Press, Princeton, New Jersey, p. 598.
- Huberty, J.M., Konishi, H., Heck, P.R., Fournelle, J.H., Valley, J.W., Xu, H., 2012. Silician magnetite from the Dales Gorge Member of the Brockman Iron Formation, Hamersley Group, Western Australia. *American Mineralogist* 97, 26–37. <http://dx.doi.org/10.2138/am.2012.3864>.
- Johnson, C.M., Beard, B.L., Klien, C., Beukes, N.J., Roden, E.E., 2008. Iron isotopes constrain biologic and abiologic processes in banded iron formation genesis. *Geochimica et Cosmochimica Acta* 72, 151–169.
- Kasting, J.F., 1987. Theoretical constraints on oxygen and carbon dioxide concentrations in the Precambrian atmosphere. *Precambrian Research* 34, 205–229.
- Kasting, J.F., 2014. Atmospheric composition of Hadean–early Archean Earth: The importance of CO. *The Geological Society of America Special Paper* 504, 19–28.
- Klien, C., Bricker, O.P., 1977. Some aspects of the sedimentary and diagenetic environment of Proterozoic banded iron formation. *Economic Geology* 72, 1457–1470.
- Konhauser, K.O., Hamade, T., Raiswell, R., Morris, R.C., Ferris, F.G., Southam, G., Canfield, D.E., 2002. Could bacteria have formed the Precambrian banded iron formations? *Geology* 30, 1079–1082.
- Konhauser, K.O., Amskold, L., Lalonde, S.V., Posth, N.R., Kappler, A., Anbar, A., 2007. Decoupling photochemical Fe(II) oxidation from shallow-water BIF deposition. *Earth and Planetary Science Letters* 258, 87–100.
- Konhauser, K.O., Pecoits, E., Lalonde, S.V., Papineau, D., Nisbet, E.G., Barley, M.E., Arndt, N.T., Zahnle, K., Kamber, B.S., 2009. Oceanic nickel depletion and a methanogen famine before the Great Oxidation Event. *Nature* 458, 750–753.
- LaBerge, G.L., 1964. Development of magnetite in iron-formations of the Lake Superior region. *Economic Geology* 59, 1313–1342.
- Li, W.Q., Huberty, J.M., Beard, B.L., Kitaa, N.T., Valley, J.W., Johnson, C.M., 2013. Contrasting behaviour of oxygen and iron isotopes in banded iron formations revealed by in situ isotopic analysis. *Earth and Planetary Science Letters* 384, 132–143.
- Moorbath, S., O’Nions, R.K., Pankhurst, R.J., 1973. Early Archaean age for the Isua iron formation, West Greenland. *Nature* 245, 138–139.
- Nutman, A.P., Allaart, J.H., Bridgwater, D., Dimroth, E., Rosing, M.T., 1984. Stratigraphic and geochemical evidence for the depositional environment of the early Archaean Isua supracrustal belt, southern West Greenland. *Precambrian Research* 25, 365–396.

- Nutman, A.P., Friend, C.R.L., Horie, H., Hidaka, H., 2007. Construction of pre-3600 Ma crust at convergent plate boundaries, exemplified by the Itsaq Gneiss Complex of southern West Greenland. In: van Kranendonk, M.J., Smithies, R.H., Bennett, V.C. (Eds.), *Earth's Oldest Rocks*. Elsevier, pp. 187–218.
- Nutman, A.P., Friend, C.R.L., Paxton, S., 2009. Detrital zircon sedimentary provenance ages for the Eoarchean Isua supracrustal belt, southern West Greenland: juxtaposition of an imbricated ca. 3700 Ma juvenile arc assemblage against an older complex with 3920–3800 Ma components. *Precambrian Research* 172, 212–233.
- Nutman, A.P., Friend, C.R.L., Bennett, V.C., Wright, D., Norman, M.D., 2010.  $\geq 3700$  Ma pre-metamorphic dolomite formed by microbial mediation in the Isua supracrustal belt (W. Greenland): simple evidence for early life? *Precambrian Research* 183, 725–737.
- Nutman, A.P., Bennett, V.C., Friend, C.R.L., Van Kranendonk, M.J., Chivas, A.R., 2016. Rapid emergence of life shown by discovery of 3,700 million year old microbial structures. *Nature* 535, 535–537. <http://dx.doi.org/10.1038/nature19355>.
- Ohmoto, H., Watanabe, Y., Kumazawa, K., 2004. Evidence from massive siderite beds for a CO<sub>2</sub>-rich atmosphere before 1.8 billion years ago. *Nature* 429, 395–399.
- Papineau, D., Mojzsis, S.J., 2006. Mass-independent fractionation of sulfur isotopes in sulphides from the pre-3770 Ma Isua Supracrustal Belt, West Greenland. *Geobiology* 4, 227–238.
- Pearce, N.J.G., Perkins, W.T., Westgate, J.A., Gorton, M.P., Jackson, S.E., Neal, C.R., Chenery, S.P., 1997. A compilation of new and published major and trace element data for NIST SRM 610 and NIST SRM 612 glass reference materials. *Geostandards Newsletter* 21 (1), 115–144.
- Pentřrkova, L., Sui, K., Pentřrk, M., Stucki, J.W., 2013. A review of microbial redox interactions with structural Fe in clay minerals. *Clay Minerals* 48, 543–560.
- Posth, N.R., Hegler, F., Konhauser, K.O., Kappler, A., 2008. Alternating Si and Fe deposition caused by temperature fluctuations in Precambrian oceans. *Nature Geoscience* 1, 703–708.
- Rasmussen, B., Meier, D.B., Krapež, B., Muhling, J.R., 2013. Iron silicate microgranules as precursor sediments to 2.5-billion-year-old banded iron formations. *Geology* 41, 435–438.
- Rasmussen, B., Muhling, J., Suvorova, A., Krapež, B., 2017. Greenalite precipitation linked to the deposition of banded iron formations downslope from a late Archean carbonate platform. *Precambrian Research* 290, 49–62.
- Rosing, M.T., Bird, D.K., Sleep, N.H., Bjerrum, C.J., 2010. No climate paradox under the faint early Sun. *Nature* 464, 744–747.
- Russell, M.J., Hall, A.J., 2006. The onset and early evolution of life. *Geological Society of America Memoir* 198, 1–32.
- Shelobolina, E., Xu, H.F., Konishi, H., Kukkadapu, Wu, T., Blöthe, M., Roden, E., 2012. Microbial lithotrophic oxidation of structural Fe(II) in biotite. *Applied and Environmental Microbiology* 78, 5746–5752.
- Siever, R., 1992. The silica cycle in the Precambrian. *Geochimica et Cosmochimica Acta* 56, 3265–3272.
- Sleep, N.H., Meibom, A., Fridriksson, Th., Coleman, R.G., Bird, D.K., 2004. H<sub>2</sub>-rich fluids from serpentinization: geochemical and biotic implications. *Proceedings of the National Academy of Sciences of the United States of America* 101, 12818–12823.
- Tosca, N.J., Stephen Guggenheim, S., Pufahl, P.K., 2016. An authigenic origin for Precambrian greenalite: implications for iron formation and the chemistry of ancient seawater. *Bulletin of the Geological Society of America* 128, 511–530.
- Van Kranendonk, M.J., Webb, G.E., Kamber, B.S., 2003. Geological and trace element evidence for marine sedimentary environment of deposition and biogenicity of 3.45 Ga stromatolite carbonates in the Pilbara Craton, and support for a reducing Archean ocean. *Geobiology* 1, 91–108.
- Whitehouse, M.J., Kamber, B.S., Fedo, C.M., Lepland, A., 2005. Integrated Pb- and S-isotope investigation of sulphide minerals from the early Archean of south-west Greenland. *Chemical Geology* 222, 112–131.